Journal of The Electrochemical Society, **161** (10) H705-H709 (2014)
0013-4651/2014/161(10)/H705/5/$31.00 © The Electrochemical Society

Correlation between Structural and Photoelectrochemical Properties of GaN Porous Nanostructures Formed by Photo-Assisted Electrochemical Etching

Yusuke Kumazaki,[z] Akio Watanabe, Zenji Yatabe, and Taketomo Sato[*]

Research Center for Integrated Quantum Electronics, and Graduate School of Information Science and Technology, Hokkaido University, Sapporo 060-8628, Japan

We investigated the correlation between structural and photoelectrochemical properties of GaN porous nanostructures formed by photo-assisted electrochemical etching. The porous nanostructures were formed during light irradiation of the top-surface of homo-epitaxial layers grown on freestanding GaN substrates. The pore depth, wall thickness, and surface morphology of porous nanostructures were strongly influenced by the way holes generated by the light irradiation were supplied. Such structural features influenced the optical properties of GaN porous nanostructures. The photoluminescence peaks measured on GaN porous nanostructures were shifted to higher energies because of the quantum confinement in the thin GaN walls between pores. Formation of porous nanostructure decreased the photoreflectance of the GaN surface, and the smallest reflectance was obtained from the porous sample having large pores on its surface after the ultrathin layer with small pores had been removed by surface-etching. The photoelectrochemical response measured on GaN porous nanostructures in a NaCl electrolyte were drastically enhanced by the unique features of those structures, such as low photoreflectance and large surface area. The largest photocurrents were obtained from the sample from which H_3PO_4 treatment had removed the ultrathin layer without thinning the pore walls.
 [DOI: 10.1149/2.1101410jes]

Manuscript submitted June 6, 2014; revised manuscript received July 24, 2014. Published August 6, 2014. This was Paper 51 presented at the San Francisco, California, Meeting of the Society, October 27-November 1, 2013.

Photoelectrochemical systems based on semiconductor photoelectrodes have recently attracted much attention due to their potential use in the next generation of green technologies such as water splitting for fuel cells, artificial photosynthesis, and so on.[1–5] Among the photoelectrode materials, GaN is one of the most attractive because of its chemical stability and its potential to achieve direct photoelectrolysis by solar power without the consumption of electric power.[6–8] In addition, the bandgap energy of GaN-based materials can be varied from about 0.65 to 6.0 eV by alloying them with InN and AlN, which enables us to design various functional photoelectrodes not only for spectral matching of solar light but also for the electrochemical reduction of CO_2 to carbohydrate.[9] One of the common approaches to improving conversion efficiency is to form nanostructures on the photoelectrode surface in order to increase its surface area. Most reported GaN nanostructures have been made using selective-area growth[10,11] or a dry etching process such as reactive ion etching.[12,13] There are, however, severe limitations on increasing the density of nanostructures because most approaches use lithography for defining the size and position of the nanostructures. And when a dry etching process is involved, the etching damage induced by ion bombardment is not negligible[14–16] and could significantly degrade the photoelectrochemical efficiency.

One alternative approach is an electrochemical-fabrication process, which can form various semiconductor nanostructures in a self-assembled fashion. The most well-known application of an electrochemical process is the formation of porous nanostructure by anodic etching in which a high-density array of nanometer- or micrometer-sized pores is formed with high productivity over a large area on the semiconductor surface.[17] We have recently reported that InP porous nanostructures showed low photoreflectance and high photoabsorption,[18,19] which are very promising features for porous nanostructures used in the photoelectric conversion devices such as photodetectors and solar cells. Besides, the electrochemical process is applicable to various semiconductors,[20–24] even chemically stable materials such as GaN,[25–29] without causing processing damage.

The electrochemical conditions including applied bias and electrolyte solutions have been investigated with regard to the formation of GaN porous nanostructures, but most of the previous studies targeted structural properties and only a few reported on the correlation between the conditions and the resultant optical properties. This is partly because the mechanism of the formation of GaN porous nanostructures has not been clarified because of sample-dependent inhomogeneity and insufficient material quality. It is well known that GaN epitaxial layer grown on sapphire substrates always have a high density of dislocations caused by strain at the lattice-mismatched interface between GaN and sapphire substrates. In such a situation, the current supply for electrochemical reactions would be strongly affected by the dislocation density and dislocation distribution of the substrates.[30] It is also difficult to judge whether the optical response obtained on sample structures is due to the intrinsic properties of GaN porous nanostructures or to photo-active dislocations in the GaN epitaxial layer.

In the work reported in this paper, we first investigated the structural properties of GaN porous nanostructures formed on n-GaN homo-epitaxial layer grown on a freestanding GaN substrate, which typically has a low dislocation density.[31] We then investigated the correlation between the structural properties and the optical properties. Optical properties of GaN porous samples were characterized by photoluminescence (PL) and photoreflectance measurements. In view of possible photoelectrode applications, the photoelectrochemical characteristics of GaN porous nanostructures were investigated using a NaCl electrolyte and comparing various samples formed under different electrochemical conditions.

Experimental

As shown schematically in Fig. 1a, n-type GaN epitaxial layers ($N_D = 2 \times 10^{16}$ cm^{-3}) grown on freestanding GaN substrates ($N_D > 1 \times 10^{18}$ cm^{-3}) were used for the electrochemical formation of GaN porous nanostructures. The threading dislocation density (TDD) of GaN substrates is approximately 2.2×10^6 cm^{-2}, which is two or three orders of magnitude less than that of hetero-epitaxial layers grown on sapphire substrates.[32] The electrochemical current was supplied through the Au-ohmic contact on the back side of the substrate, and the electrochemical process was performed using a standard cell with three electrodes: an n-type GaN working electrode, a Pt counter electrode, and a Ag/AgCl reference electrode (see Fig. 1b). We used a mixture of 1 mol/L H_2SO_4 and 1 mol/L H_3PO_4 (pH = 2.5) as an electrolyte to remove resulting oxides and expose the raw GaN surface for further etching.[29] Xe lamp was the light source in the photo-assisted electrochemical etching forming GaN porous nanostructures.

Typical cyclic voltammograms of an n-GaN epitaxial layer that were obtained at light intensities P_{IN} between 0 and 40 mW/cm^2 by

[*]Electrochemical Society Active Member.
[z]E-mail: kumazaki@rciqe.hokudai.ac.jp

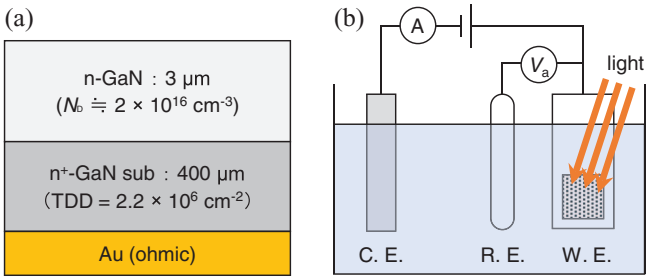

Figure 1. Schematic illustrations of (a) device structure and (b) electrochemical cell.

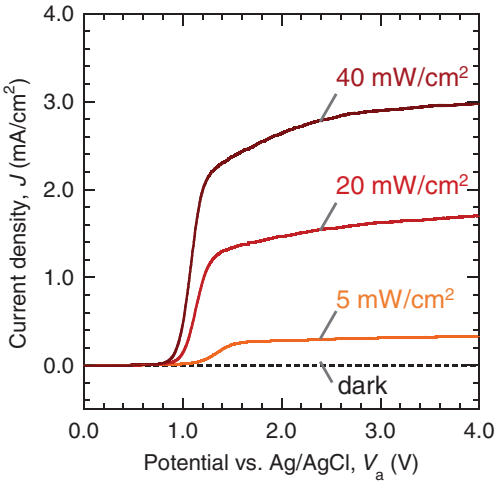

Figure 2. Cyclic voltammograms measured on as-grown GaN electrode under light irradiation with various P_{IN}.

sweeping the potential V_a between 0 and 4.0 V are shown in Fig. 2. Little or no current was measured in the dark because of the absence of holes in the n-GaN layer. Under light irradiation, on the other hand, current started to flow at about 1.0 V. Higher currents were measured at higher light intensities, and these currents resulted in anodization of the n-GaN surface. We therefore tried to form porous nanostructures under irradiation; that is, by photo-assisted electrochemical etching. In view of low-energy processing as a first attempt, V_a was set at 1.0 V and P_{IN} was set at 5 mW/cm^2. The structural characteristics were investigated by scanning electron microscopy (SEM) using a Hitachi SU-8010 system. PL measurements were carried out using an optical multichannel analyzer system (Acton Research Corporation) and a He-Cd laser with an intensity of 0.05 mW/cm^2 at a wavelength λ of 325 nm. Photoreflectance properties were investigated using a Bunko-Keiki CEP-25SR system in the diffuse-reflectance configuration. Photoelectrochemical characterization of various porous samples was conducted using a setup similar to that used for the formation of porous nanostructure (Fig. 1b). Photocurrents of GaN porous electrodes were measured in 1 mol/L NaCl (pH = 7.0) under light irradiation with wavelength λ = 350 nm and P_{IN} = 0.1 mW/cm^2.

Results and Discussion

Figures 3 show the top and cross-sectional SEM images of GaN porous samples formed at V_a = 1.0 V, P_{IN} = 5.0 mW/cm^2, and various anodization times t_a: (a) t_a = 300 s (sample A), (b) t_a = 600 s (sample B), (c) t_a = 1800 s (sample C), and (d) t_a = 600 s with a chemical treatment (the process used to form sample B′ will be described later). The pore density formed on the surface was estimated from SEM images to be about 10^{10} cm^{-2}, which is much higher than the dislocation density of the substrates. This suggests that the pore formation in this study was substantially unaffected by the dislocations in GaN substrates. In the cross-sectional views of samples A and B we can clearly see pores with diameters over 30 nm, and in the top views we can see pores with diameters under 10 nm. These results suggest that an ultrathin porous layer having smaller-diameter pores formed on top of a thick porous layer having larger-diameter pores. Figure 4 shows the relationship between pore depth d_p and the charge density Q passing through the working electrode during the anodization. The d_p increased with Q, and the slope of the experimental curve decreased gradually. This gradual decrease indicates that the rate of pore formation in the depth direction decreased with increasing Q. Considering the proportional relationship between the amount of electrochemical reaction and Q, as described by Faraday's law, the decreased slope shown in Fig. 4 indicates that lateral etching of pore walls occurred in addition to the vertical etching in the depth direction.

As shown in Fig. 3c, on the other hand, the structural features of sample C, formed at t_a = 1800 s, differ from those of samples A and B. In the top view, we can clearly see pores over 30 nm in diameter, and in the cross-sectional view, we can see no ultrathin porous layer with smaller pores. Furthermore, as shown in Fig. 4, the d_p in sample C was smaller than that in samples formed at shorter t_a and smaller Q. These results indicate that surface etching as well as vertical etching in the depth direction occurred.

We considered the mechanism of GaN porous nanostructure formation by referring to the "Beale model" proposed for porous Si

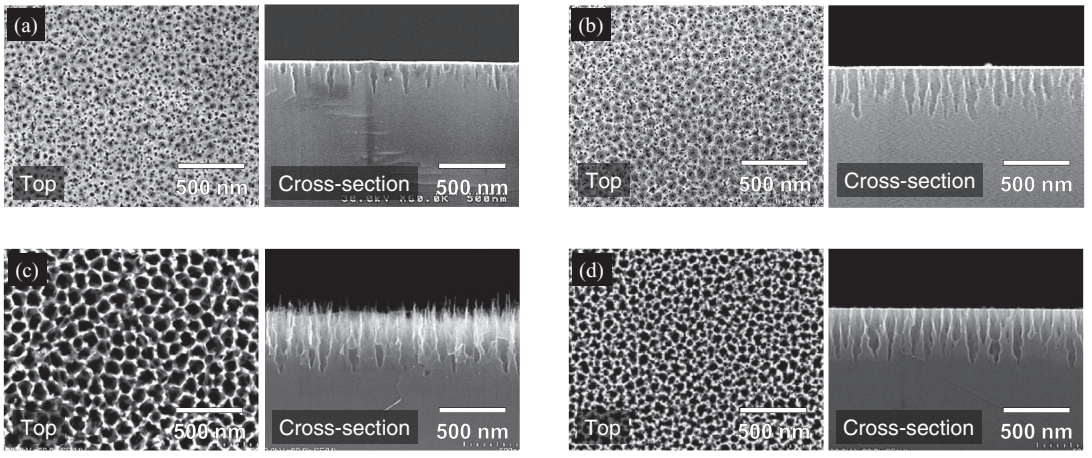

Figure 3. Top and cross-sectional SEM images of GaN porous nanostructures formed by photo-assisted electrochemical etching at V_a = 1.0 V, P_{IN} = 5 mW/cm^2, and various t_a: (a) t_a = 300 s (sample A), (b) t_a = 600 s (sample B), (c) t_a = 1800 s (sample C), and (d) t_a = 600 s after H_3PO_4 treatment (sample B′).

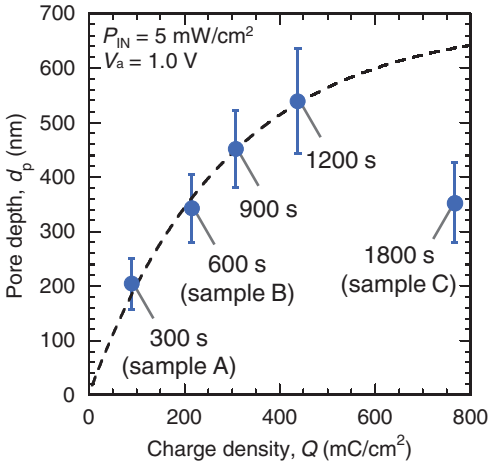

Figure 4. Pore depth as a function of charge density Q.

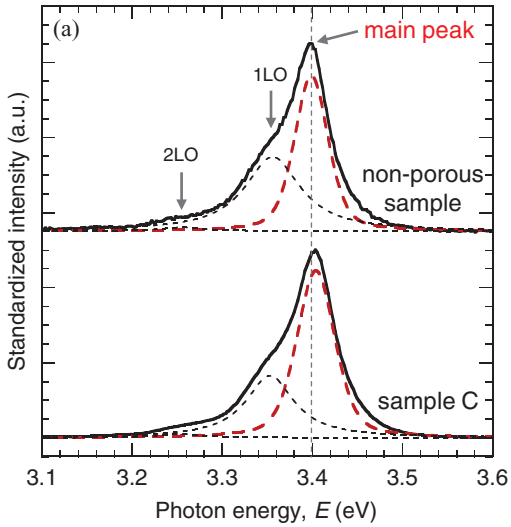

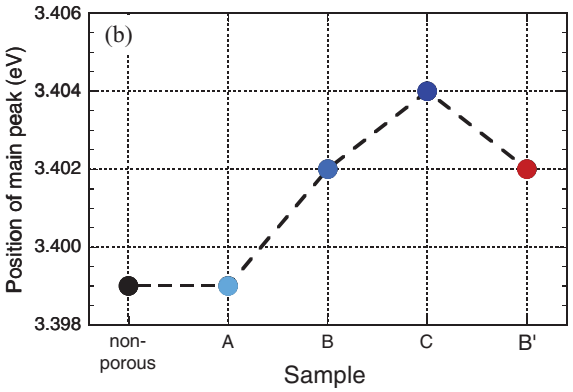

Figure 6. (a) PL spectra obtained at room temperature from a non-porous sample and porous sample C formed at t_a = 1800 s, and (b) PL peak positions of porous samples and a non-porous sample.

nanostructures.[33,34] Figure 5 shows the formation flow for GaN porous nanostructures schematically. At the initial stage, photo-generated holes transferred preferentially to the pore tips at which electric field lines concentrated, leading to the formation of porous nanostructures ((a) → (b)). Since the holes generated near the surface also transferred to the pore walls, etching of pore walls and the top-surface occurred in addition to the vertical etching at the pore tips ((b) → (c)). After reaching a critical depth, etching proceeded preferentially at the top-surface removing the ultrathin porous layer with smaller size pore ((c) → (d)), resulting in larger pores observed in sample C. There are two possible reasons for this phenomenon. One is due to the reduced diffusion of ions to pore tips in deeper pores, and another is due to the decreased hole-supply to pore tips. A similar preferential top-surface etching is also observed on InP porous nanostructures under irradiation.[35] This formation model can compatibly explain both the SEM results in Figs. 3a–3c and the correlation between pore depth and Q shown in Fig. 4.

The correlation with the crystal quality such as a dislocation density has been frequently reported in the chemical and electrochemical etching. A previous study[36] found that photo-assisted electrochemical etching of GaN layers occurred only at dislocation-free areas because the dislocations acted as recombination centers for the photo-generated carries. Another study[37] found that the etching using a HF solution proceeds thorough the dislocations and grain boundaries, whereas the etching using a KOH solution takes place at crystal grains. These reports showed that the etching profile was strongly affected by the dislocation density and distribution in GaN layers. However, that was not the case with this study. The TDD of the GaN epitaxial layer used in this study is 2.2×10^6 cm^{-2}, which means approximately 1 dislocation in 5 μm^2. The pore density of the present GaN porous nanostructures, however, is estimated to be over 5000 pores per 5 μm^2. This fact indicates that the formation model proposed here is acceptable for the present study free of influence from the dislocations in GaN layers.

The correlation between the structural properties and optical properties was investigated in the photoluminescence and photoreflectance measurements conducted on the GaN porous samples shown in Figs. 3a–3d. As for sample B′ shown in Fig. 3d, the ultrathin porous layer with smaller pores was removed by immersing the sample in a heated H_3PO_4 solution for 1 min after the formation of porous nanostructure with t_a = 600 sec. Figure 6a shows PL spectra obtained at room temperature from a non-porous sample and porous sample C formed at t_a = 1800 s. Both samples exhibited strong near-band-edge

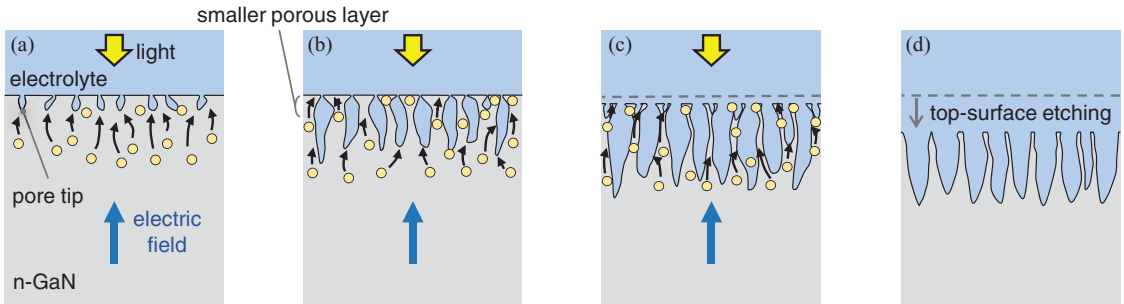

Figure 5. Model of GaN porous nanostructure formation by photo-assisted electrochemical etching.

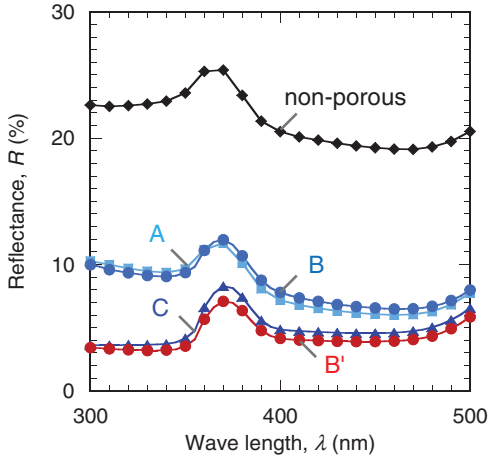

Figure 7. Diffuse reflectance spectra of non-porous and porous GaN: sample A formed at $t_a = 300$ s, sample B formed at $t_a = 600$ s, sample C formed at $t_a = 1800$ s, and sample B′ formed at $t_a = 600$ s after H_3PO_4 treatment.

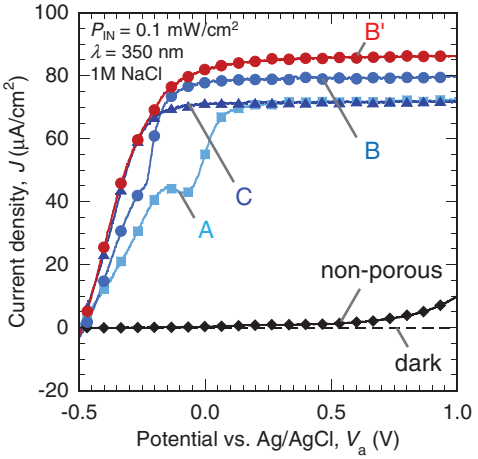

Figure 8 Photoelectrochemical characteristics of non-porous and porous GaN: sample A formed at $t_a = 300$ s, sample B formed at $t_a = 600$ s, sample C formed at $t_a = 1800$ s, and sample B′ formed at $t_a = 600$ s after H_3PO_4 treatment.

emission around 3.4 eV with a full width at half maximum (FWHM) of ∼50 meV. In the present samples, two additional peaks related to longitudinal optical (LO) phonon replicas were also observed. The position of main peak obtained from sample C is at 3.404 eV which is about 5 meV higher than that of the main peak obtained from the non-porous sample. We believe that the observed blueshift is most probably due to the quantum confinement in pore walls, similarly to the case of porous Si[38] and InP.[39] The quantum confinement energy in GaN walls was calculated by assuming a vacuum/GaN quantum well, whose thickness corresponds to the wall thickness t_w as follows.

$$\Delta E = \frac{h^2}{8{t_w}^2}\left(\frac{1}{{m_e}^*} + \frac{1}{{m_h}^*}\right), \qquad [1]$$

where h is Planck's constant, ${m_e}^*$ and ${m_h}^*$ are masses of electron and hall of GaN, respectively. According to Eq. 1, a peak shift of 5 meV would be caused when the thickness of pore walls was about 21 nm. This estimated thickness is very consistent with the thickness measured in SEM observation. The positions of the main peaks obtained from all porous samples are summarized in Fig. 6b. The peak position of sample A was almost same with that of the non-porous sample. The peak positions of samples B and C, on the other hand, shifted higher position with increasing t_a. This result suggests that the effect of the quantum confinement increased in the pore walls being thinner with increase of t_a. It is to be also noted that the peak position of sample B′, whose ultrathin porous layer was removed by a H_3PO_4 treatment, is the same as that of sample B formed with $t_a = 600$ s. As shown in Fig. 3 pores over 30 nm in diameter were seen in top views of sample B′, whereas there was almost no difference between the features seen in cross-sectional views of samples B and B′. These results show that the H_3PO_4 treatment removed the ultrathin porous layer with smaller pores without thinning the pore walls.

Figure 7 shows diffuse reflectance spectra of porous samples and a non-porous sample measured as a reference. As expected, the photoreflectance R of all porous samples was lower than that of the non-porous sample. The porous samples could be separated into two groups according to reflectance value: a higher-R group comprising samples like A and B, and a lower-R group comprising samples like C and B′. SEM observation of the porous samples shown in Figs. 3a–3d revealed that the photoreflectance depends more on surface morphology than pore depth. Comparing sample B′ with sample B, one sees the reflectance surface etching using a chemical treatment decreased reflectance even though the electrochemical conditions forming porous nanostructure were the same for both samples. This phenomenon is very similar to the case of InP porous nanostructures.[19] In samples C and B′, pores with enlarged openings appeared on the surface, where air holes are closely aligned between the thin GaN walls. This kind of air-dielectric composite has a refractive index n close to unity, leading to low reflectance at the air interface.

Photoelectrochemical characteristics of various GaN porous nanostructures were measured in 1 mol/L NaCl electrolyte under irradiation with monochromatic light ($\lambda = 350$ nm, $P_{IN} = 0.1$ mW/cm^2). Figure 8 compares the photocurrent-voltage curves obtained on porous samples and the non-porous sample. No current degradation or structural change was observed in repeated experiments because oxidation of the GaN surface was suppressed oxidation in the Cl^--containing electrolyte.[6] Here, the dominant electrochemical reactions in this system are thought here to be due to the photo-assisted electrolysis of water, the reduction of H^+, and the oxidation of Cl^-. As shown in Fig. 8, the photocurrents of all porous samples increased much more than did the photo-current of the non-porous sample. External quantum efficiency η can be calculated by

$$\eta = \frac{hc\left|J_{ph} - J_{dark}\right|}{q\lambda P_{IN}}, \qquad [2]$$

where h is Planck's constant, c is speed of light, q is elementary charge, J_{ph} and J_{dark} are current density under irradiation and dark condition, respectively. From the calculations using Eq. 2, it was found that η of the non-porous sample was very low, i. e., only 0.001% at 0 V and 0.332% at 1.0 V applied bias. After the formation of porous structures, however, η were drastically enhanced to as high as 2.926% at 0 V. This might be due to the unique features of porous nanostructures, such as their large surface area and low reflectance. These results enable us to conclude that the formation of porous nanostructures is effective for improving photoelectrochemical characteristics and is a promising technique for use in photoelectrochemical water splitting.

It was also found that the photoelectrochemical characteristics were greatly influenced by the structural variations of porous samples. Structural and optical properties of porous samples are listed in Table I. Photocurrents of sample B were larger than those of sample A. Since the most apparent difference between sample A and B was pore

Table I. Structural and optical properties of porous samples.

Sample	Pore depth d_p (nm)	PL peak shift (meV)	Photoreflectance R (%)	Photocurrent density J_{ph} (μA/cm^2)
A	200	0	9.6	55.3
B	340	3.0	9.4	77.7
C	350	5.0	4.1	71.2
B′	340	3.0	3.5	82.7

depth, it would appear that the improved photoelectrochemical characteristics of sample B were due to its increased pore depth increasing the pores′ contribution to the sample's surface area. On the other hand, the photocurrents of sample C were lower than those of sample B in spite of the pore depths of the two samples being almost the same. One possible reason for this is the thinning of the pore walls in sample C. As described above, the thickness of pore wall decreased during the prolonged process with $t_a = 1800$ s. The thinning of the pore walls probably decreased thickness of photoabsorption region in the pore walls, and/or degraded carrier transport properties by increasing resistivity.

The photocurrent of sample B which is the highest among porous samples A–C was furthermore improved by H_3PO_4 treatment as observed at sample B′. SEM observation and photoreflectance measurements revealed that its lower reflectance after the removal of ultrathin porous layer was obtained without thinning the pore walls. The typical relationship between photoreflectance R and photocurrent J_{ph} is expressed by

$$J_{ph} \propto \phi_{IN}(100 - R), \quad [3]$$

where ϕ_{IN} is the irradiated photon flux. Assuming that the material properties of sample B and B′ are the same, we have the following equation:

$$\frac{J_{ph(B')}}{J_{ph(B)}} = \frac{100 - R_{(B')}}{100 - R_{(B)}}. \quad [4]$$

Substituting the values obtained in this study to Eq. 4, we obtained almost equal values of 1.06 and 1.07, respectively, for the left hand side and right hand side of the equation. Accordingly, the increase of photocurrent by H_3PO_4 treatment could be explained by the effect of the decrease of photoreflectance in Eq. 4. In such a situation, the number of photons absorbed at pore walls increased, resulting in the improvement of photoelectrochemical conversion efficiency. These results indicate that the control of porous nanostructures features such as surface morphology, thickness of pore walls, and pore depth is crucial to the improvement of the photoelectrochemical characteristics of GaN porous nanostructures.

Conclusions

Porous nanostructures were formed on n-GaN homo-epitaxial layers by using photo-assisted electrochemical etching. From SEM observations, it was found that the way holes were generated by the light irradiation played a key role in determining the pore depth, wall thickness, and surface morphology of GaN porous nanostructures. Under light irradiation of the top-surface, the pore diameter increased with the anodization time t_a because of the preferential etching of pore walls on the top surface. PL measurements revealed that the wall thickness decreased with increasing t_a, which is very consistent with the results of SEM observation. Formation of porous nanostructure decreased the photoreflectance of the GaN surface, and the smallest reflectance was obtained from the porous sample having large pores on the surface after the ultrathin layer with small pores had been removed by surface-etching. The photoelectrochemical responses measured on GaN porous nanostructures in a NaCl electrolyte were drastically enhanced by the unique features of those structures, such as low photoreflectance and large surface area. From the comparison of various porous samples it was found that the largest photocurrents were obtained on the sample from which H_3PO_4 treatment had removed the ultrathin layer without thinning the pore walls. These results indicate that GaN porous nanostructures formed by the photo-assisted electrochemical etching are very promising for use as the photoelectrochemical electrodes expected to play a role in the next-generation green technologies.

Acknowledgments

This work was supported in part by a grant-in-Aid for Scientific Research (B) – 25289079 from Japan Society for the Promotion of Science (JSPS).

References

1. A. Fujishima and K. Honda, *Nature* **238**, 37 (1972).
2. K. Maeda, K. Teramura, D. L. Lu, T. Takata, N. Saito, Y. Inoue, and K. Domen, *Nature* **440**, 295 (2006).
3. E. E. Barton, D. M. Rampulla, and A. B. Bocarsly, *Journal of the American Chemical Society* **130**, 6342 (2008).
4. S. Sato, T. Arai, T. Morikawa, K. Uemura, T. M. Suzuki, H. Tanaka, and T. Kajino, *Journal of the American Chemical Society* **133**, 15240 (2011).
5. B. Oregan and M. Gratzel, *Nature* **353**, 737 (1991).
6. I. M. Huygens, K. Strubbe, and W. P. Gomes, *Journal of the Electrochemical Society* **147**, 1797 (2000).
7. J. D. Beach, R. T. Collins, and J. A. Turner, *Journal of the Electrochemical Society* **150**, A899 (2003).
8. K. Fujii, T. K. Karasawa, and K. Ohkawa, *Japanese Journal of Applied Physics Part 2-Letters & Express Letters* **44**, L543 (2005).
9. S. Yotsuhashi, M. Deguchi, Y. Zenitani, R. Hinogami, H. Hashiba, Y. Yamada, and K. Ohkawa, *Applied Physics Express* **4**, 117101 (2011).
10. Y. D. Wang, K. Y. Zang, and S. J. Chua, *Journal of Applied Physics* **100**, 054306 (2006).
11. I. Waki, D. Cohen, R. Lal, U. Mishra, S. P. DenBaars, and S. Nakamura, *Applied Physics Letters* **91**, 093519 (2007).
12. H. Ono, Y. Ono, K. Kasahara, J. Mizuno, and S. Shoji, *Japanese Journal of Applied Physics* **47**, 933 (2008).
13. W. M. Zhou, G. Q. Min, Z. T. Song, J. Zhang, Y. B. Liu, and J. P. Zhang, *Nanotechnology* **21**, 405304 (2010).
14. E. D. Haberer, C. H. Chen, A. Abare, M. Hansen, S. Denbaars, L. Coldren, U. Mishra, and E. L. Hu, *Applied Physics Letters* **76**, 3941 (2000).
15. R. Dimitrov, V. Tilak, W. Yeo, B. Green, H. Kim, J. Smart, E. Chumbes, J. R. Shealy, W. Schaff, L. F. Eastman, C. Miskys, O. Ambacher, and M. Stutzmann, *Solid-State Electronics* **44**, 1361 (2000).
16. F. A. Khan, L. Zhou, V. Kumar, and I. Adesida, *Journal of Vacuum Science & Technology B* **19**, 2926 (2001).
17. A. Uhlir, *Bell System Technical Journal* **35**, 333 (1956).
18. Y. Kumazaki, T. Kudo, Z. Yatabe, and T. Sato, *Applied Surface Science* **279**, 116 (2013).
19. T. Sato, N. Yoshizawa, and T. Hashizume, *Thin Solid Films* **518**, 4399 (2010).
20. V. Lehmann, *Journal of the Electrochemical Society* **140**, 2836 (1993).
21. X. G. Zhang, *Journal of the Electrochemical Society* **151**, C69 (2004).
22. B. H. Erne, D. Vanmaekelbergh, and J. J. Kelly, *Journal of the Electrochemical Society* **143**, 305 (1996).
23. W. Shin, T. Hikosaka, W. S. Seo, H. S. Ahn, N. Sawaki, and K. Koumoto, *Journal of the Electrochemical Society* **145**, 2456 (1998).
24. T. Sato, T. Fujino, and T. Hashizume, *Electrochemical and Solid State Letters* **10**, H153 (2007).
25. A. P. Vajpeyi, S. J. Chua, S. Tripathy, and E. A. Fitzgerald, *Applied Physics Letters* **91**, 083110 (2007).
26. H. Hartono, C. B. Soh, S. J. Chua, and E. A. Fitzgerald, *Journal of the Electrochemical Society* **154**, H1004 (2007).
27. D. T. Chen, H. D. Xiao, and J. Han, *Journal of Applied Physics* **112**, 064303 (2012).
28. K. Al-Heuseen, M. R. Hashim, and N. K. Ali, *Journal of the Electrochemical Society* **158**, D240 (2011).
29. K. P. Beh, F. K. Yam, L. K. Tan, S. W. Ng, C. W. Chin, and Z. Hassan, *Japanese Journal of Applied Physics* **52**, 08JK03 (2013).
30. D. Zhuang and J. H. Edgar, *Materials Science & Engineering R-Reports* **48**, 1 (2005).
31. Y. Oshima, T. Eri, M. Shibata, H. Sunakawa, K. Kobayashi, T. Ichihashi, and A. Usui, *Japanese Journal of Applied Physics Part 2-Letters* **42**, L1 (2003).
32. P. Visconti, K. M. Jones, M. A. Reshchikov, R. Cingolani, H. Morkoc, and R. J. Molnar, *Applied Physics Letters* **77**, 3532 (2000).
33. M. I. J. Beale, N. G. Chew, M. J. Uren, A. G. Cullis, and J. D. Benjamin, *Applied Physics Letters* **46**, 86 (1985).
34. V. Lehmann and H. Foll, *Journal of the Electrochemical Society* **137**, 653 (1990).
35. T. Sato and A. Mizohata, *Electrochemical and Solid State Letters* **11**, H111 (2008).
36. C. Youtsey, L. T. Romano, and I. Adesida, *Applied Physics Letters* **73**, 797 (1998).
37. C. B. Soh, C. B. Tay, R. J. N. Tan, A. P. Vajpeyi, I. P. Seetoh, K. K. Ansah-Antwi, and S. J. Chua, *Journal of Physics D-Applied Physics* **46**, 365102 (2013).
38. L. T. Canham, *Applied Physics Letters* **57**, 1046 (1990).
39. T. Fujino, T. Sato, and T. Hashizume, *Japanese Journal of Applied Physics Part 1-Regular Papers Brief Communications & Review Papers* **46**, 4375 (2007).